Electronic Supplementary Material (ESI) for New Journal of Chemistry.

Supporting Information

Superb-selective Chemodosimetric Signaling of Sulfide in Absence and in Presence of CT-DNA and Imaging in Living Cells by Plant Alkaloid Berberine Analogue

Gopal Chandra Jana[a], Munira Khatun[a], Sk Nayim[a], Somnath Das[a], Anukul Maji[a], Maidul Beg[a], Anirudha Patra[a], Paromita Bhattacharjee[b], Kakali Bhadra[b] and Maidul Hossain*[,a]

[a]Department of Chemistry and Chemical Technology, Vidyasagar University, Midnapore-721102, West Bengal, India.

[b]Department of Zoology, University of Kalyani, Kalyani-741235, West Bengal, India.

Corresponding author: Dr. Maidul Hossain[a], Assistant Professor, Department of Chemistry and Chemical Technology, Vidyasagar University, Midnapore, 721102, West Bengal, India. Mobile no: 9432976277. Email address: hossainm@mail.vidyasagar.ac.in

CT-DNA binding affinities studies by spectroscopic analysis

Absorption Spectral Studies

The binding of BER-S with CT-DNA was mostly investigated by absorption spectroscopy titration methodology. The analogue, like berberine,has characteristic absorption in the region 300- 600 nm while in this region DNA has negligible absorbance which offers to scrutinize the DNA binding affinity of the derivative.

The absorbance titration spectrum of BER-S with increasing concentration of CT DNA up to saturation and corresponding Scatchard plot was depicted in Fig. S1a. In this titration, a significant bathochromic (342 nm to 347 nm) and hypochromic shifts (30.85%) were observed with clearly visible three isosbestic points which revealed strong intermolecular association. The parent berberine along with the substituent moiety enters into the DNA helix in such way that it was unable to form H-bonds with solvent molecule, but the strong interaction between π e^-cloud of the interacting analogue and DNA base pairs occurred which lead such type of spectral change stated above. The presence of sharp isosbestic point is a sign of equilibrium binding and also indicates the coexistence of two systems consisting of only free and bound alkaloid at any particular wavelength. The Scatchard plots of r/C_f vs. r (Fig. S1a, inset), where r is the number of moles of alkaloid bound per mole of DNA and consequent McGhee-von Hippel analysis of spectrophotometric data revealed that binding of BER-S with DNA was non-cooperative as ascribed by the negative slope with respect to r values. The intrinsic binding affinity (K_i), numbers of base pair excluded by the binding of single alkaloid molecules (n) were obtained by analysis of McGhee Von Hippel non-cooperative model of binding (Table-S2, ESI†).

Emission Spectral Studies

Berberine was weak fluorescence properties and, like berberine, our synthesized analogue BER-S was also a weak fluorophore with emission maximum around 490 nm when excited 360 nm. Accordingly, upon excitation at 360nm, the emission maxima shifted surprisingly from 490 nm to 530 nm, and fluorescence intensity increased remarkably upon binding with DNA up to saturation (Fig. S1b). Such massive shifting in emission maxima around 40 nm with enhanced intensity indicated the weakening of the electronic structure of BER-S, and due to this, the effective overlap of π electron cloud between BER-S and DNA occurred. As a result, the analogue bounded to DNA with higher affinity. The intrinsic binding affinity (K_i), numbers of base pair excluded by the binding of single alkaloid molecule (n) from fluorescence data were obtained by analysis of McGhee Von Hippel non-cooperative model of binding (Fig. 3b, inset). The optical properties (absorption and emission) of BER-S in free and DNA binding situation are described in Table-S1 (ESI†). The binding constant and n value of fluorescence studies were very similar to those obtained from spectrophotometric studies (Table-S2, ESI†).

Elucidation of the mode of binding of the analogue BER-S

By fluorescence quenching method

In the fluorescence quenching method, an anionic quencher, ferrocyanide ion was used to distinguish between intercalation and groove binding modes of berberine analogue. The ferrocyanide ion would not be able to penetrate the DNA helix as both were negatively charged. Accordingly, if the analogues are bound inside the DNA helix by intercalation, fluorescence quenching spectra is more or less same.

The Stern-Volmer plot for fluorescence quenching of BER-S-DNA complex by ferrocyanide ion is presented in (Fig. S2a). The results indicated that free derivative molecule (Ksv = 115 M^{-1}) as well as was BER-S-DNA complex (Ksv = 115 M^{-1}) quenched more effectively by ferrocyanide ion. The substituent 2, 4-dinitrosulfonyl group at 9 positions appears to be too close the isoquinoline moiety of berberine leading to inhibition of the intercalation of the analogue, BER-S. For that reason, the mode of binding of synthesized alkaloid to CT-DNA was mainly groove binding.

By viscosity measurement

Even though various spectroscopic experiments offer much significant information relating to BER-S-DNA interaction, but not adequate clues to verify how the BER-S interacts with CT-DNA, i.e., the binding approach. From the figure it is shown that $(\eta/\eta_0)^{1/3}$ of DNA remains almost same upon addition of BER-S whereas the said value increased remarkably on adding ethidium bromide (EtBr), classical intercalators to DNA solution (Fig. S2b). This result further clarified that the synthesized probe BER-S is a groove binding drug towards CT-DNA as we obtained from quenching study.

Table S1: Summary of optical properties of free and CT-DNA bounded BER-S(3).

Absorbance		Emission	
λmax (free)/nm	342	λmax (free)/nm	490
λmax (bound)/nm	347	λmax (bound)/nm	530
λiso[b]	362,379,473	F_b/F_0[a]	12.73
ε_f (atλmax)/ $M^{-1}cm^{-1}$	19,000		
ε_b (atλmax)/ $M^{-1}cm^{-1}$	12,471		
ε_{iso}(at λiso)/ $M^{-1}cm^{-1}$	9,061		

[(a)] $F_0$and F_b is the emission intensities of the free and wholly bound BER-S at 530 nm.

Table S2: Comparative binding aspects of BER-S in from absorption and emission studies

Absorption spectroscopy		Emission spectroscopy	
Binding constant (k)	No. of excluded base pair (n)	Binding constant (k)	No. of excluded base pair (n)
3.49×10^5	12.10	3.64×10^5	11.56

Table-S3: Fluorescence quantum yield (Φ) of the reactant and product (with and without DNA)

Entry	Quantum yield (ϕ)
BER-S in absence of DNA	0.0005
BER-S in presence of DNA	0.006
BER-OH in absence of DNA	0.005
BER-OH in presence of DNA	0.02

Images of CT-DNA binding studies:

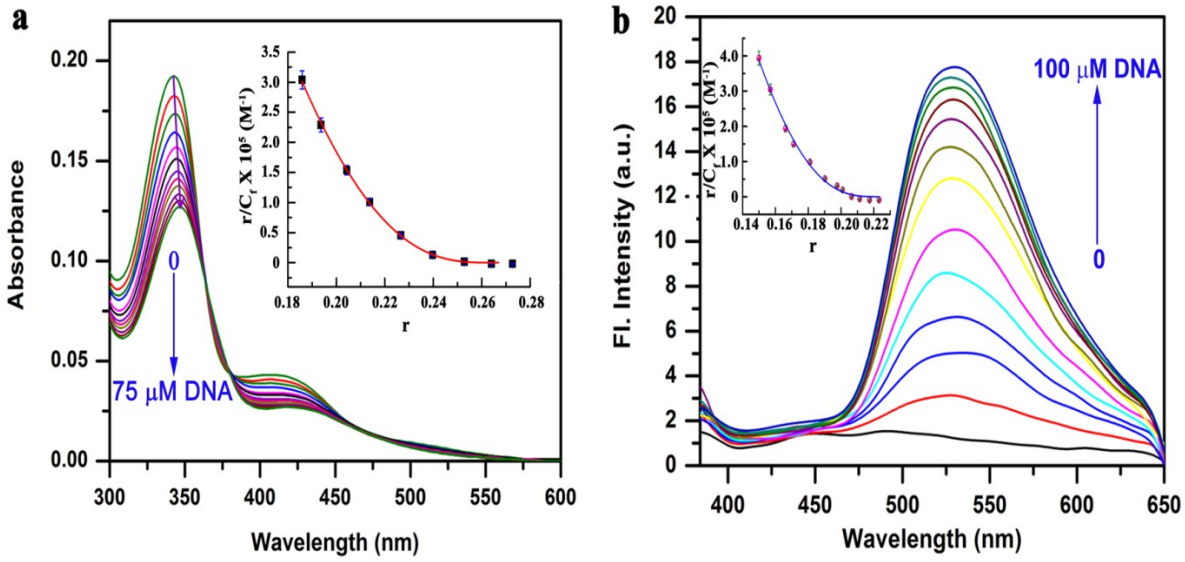

Fig. S1 (a) UV-vis spectral changes in BER-S (10μM) with increasing concentration of DNA up to 75 μM in CP buffer and Scatchard plot for the binding obtained from McGhee-von Hippel analysis of spectrophotometric data (inset). (b) Fluorescence spectra of BER-S(10 μM) with increasing concentration of DNA up to 100 μM of DNA in CP buffer solution, λex= 360 nm, λem= 530 nm and Scatchard plot for the binding constant obtained from McGhee-von Hippel analysis of spectrofluorimetric data (inset).

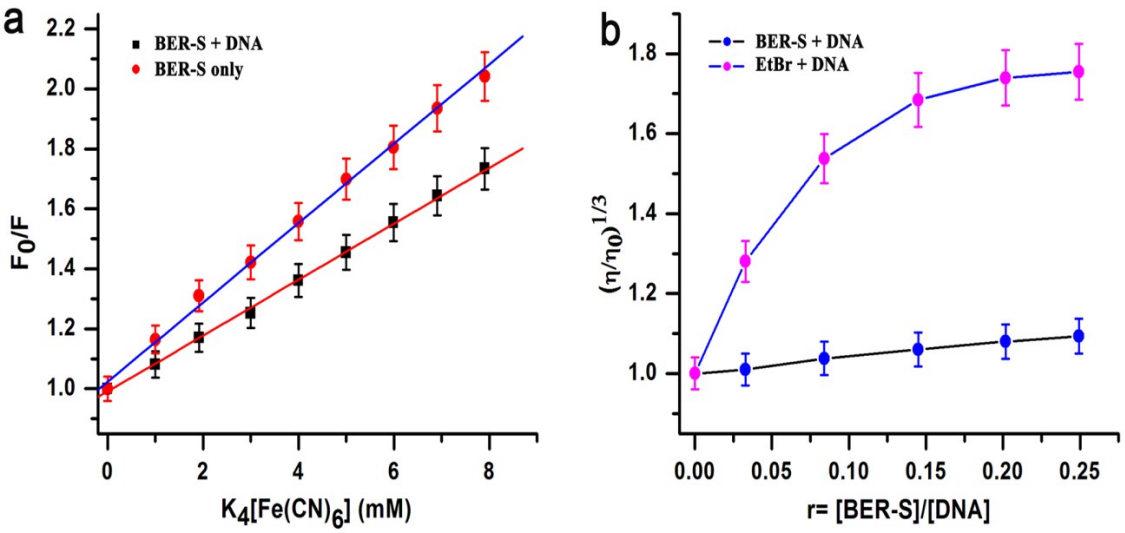

Fig. S2 (a) Stern-Volmer plots for quenching fluorescence intensity of BER-S by increasing concentration of $[Fe(CN)_6]^{4-}$ in the absence and in the presence of CT DNA in 10 mM CP buffer, pH 7.2 at 20°C.(b) Relative viscosity $(\eta/\eta_0)^{1/3}$ of CT-DNA (1 mM) in buffer solution in the presence of increasing amounts of [BER-S].

Images of colorimetric sensing of S2- by BER-S:

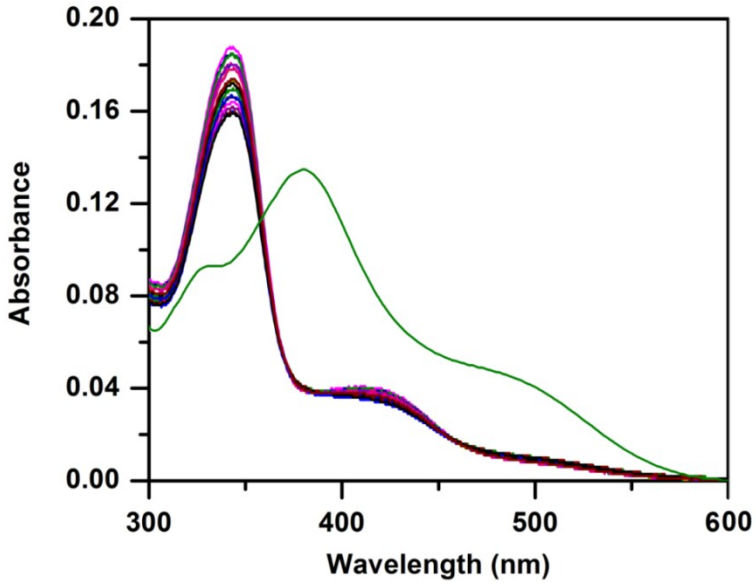

Fig. S3 UV-vis spectra of BER-S(10μM) in the presence of various analytes (25 μM for each, sulfide, Cl^-, Br^-, I^-, F^-, Ac^-, NO_2^-, NO_3^-, CN^-, SCN^-, HSO_3^-, SO_4^{2-}, SO_3^{2-}, $S_2O_3^{2-}$, $S_2O_8^{2-}$, HPO_4^{2-}, $H_2PO_4^-$, PO_4^{3-}, ClO_4^-, IO_4^-, $S_2O_8^{2-}$, BO_3^{3-}, $B_4O_7^{2-}$, N_3^-) in CP buffer solution, measured after 25 min of mixing.

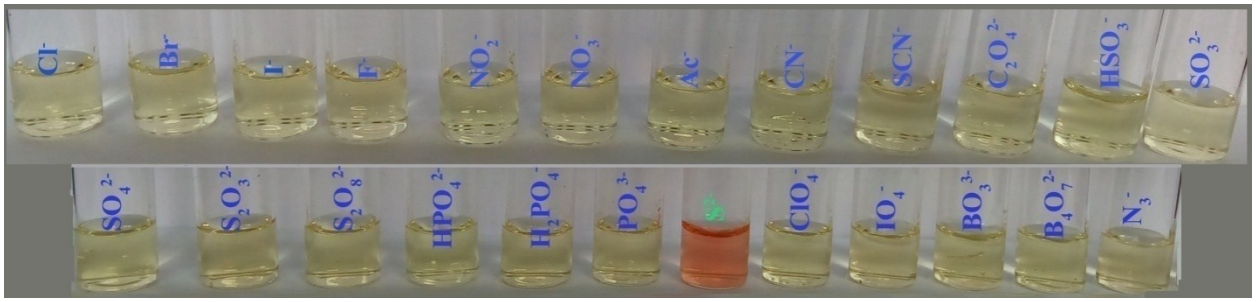

Fig. S4 The color change of BER-S (10μM) with various analytes (25μM). The pictures were recorded at 25 min after addition of the analytes (S^{2-}, Cl^{-}, Br^{-}, I^{-}, F^{-}, Ac^{-}, NO_2^{-}, NO_3^{-}, $C_2O_4^{2-}$, CN^{-}, SCN^{-}, HSO_3^{-}, SO_4^{2-}, SO_3^{2-}, $S_2O_3^{2-}$, $S_2O_8^{2-}$, HPO_4^{2-}, $H_2PO_4^{-}$, PO_4^{3-}, ClO_4^{-}, IO_4^{-}, $S_2O_8^{2-}$, BO_3^{3-}, $B_4O_7^{2-}$, N_3^{-}).

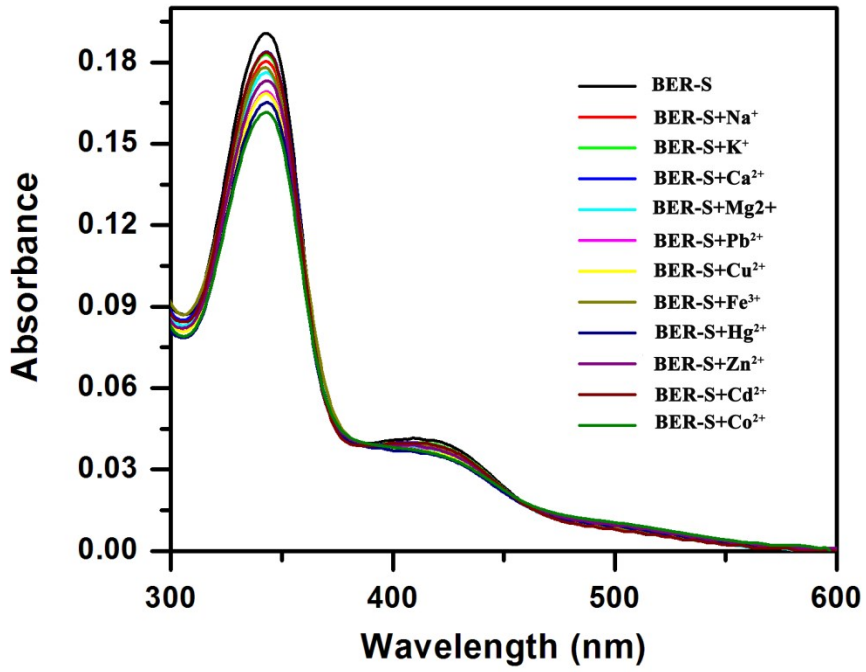

Fig. S5 UV-vis spectra of BER-S(10μM) in the presence of various analytes (25 μM for each, Na^{+}, K^{+}, Ca^{2+}, Mg^{2+}, Pb^{2+}, Cu^{2+}, Fe^{3+}, Hg^{2+}, Zn^{2+}, Cd^{2+}, Co^{2+}) in CP buffer solution, measured after 25 min of mixing.

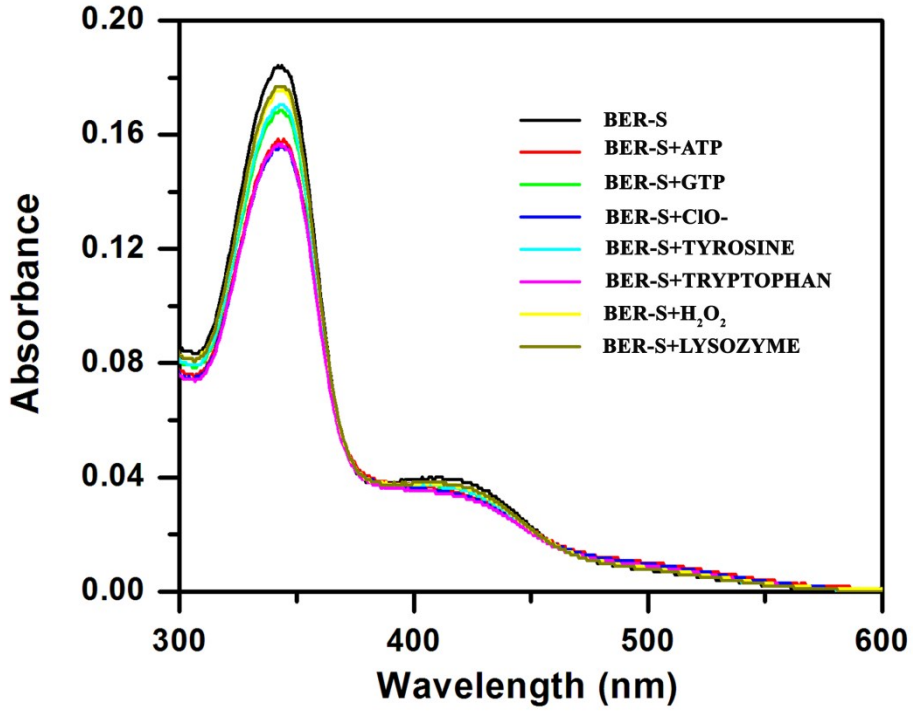

Fig. S6 UV-vis spectra of BER-S (10μM) in the presence of various analytes (25 μM for each, ATP, GTP, ClO^-, H_2O_2, tyrosine, tryptophan, lysozyme) in CP buffer solution, measured after 25 min of mixing.

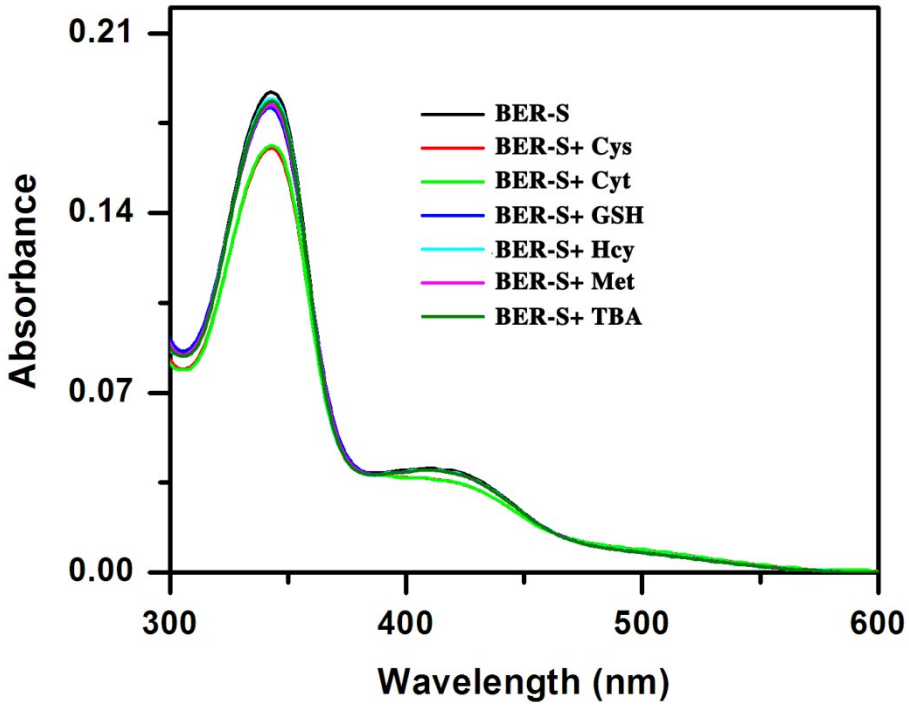

Fig. S7 UV-vis spectra of BER-S(10μM) in the presence of various biothiols (25 μM for cysteine, homocysteine, glutathione, methionine, cysteamine and thiobarbituric acid) in CP buffer solution, measured after 25 min of mixing.

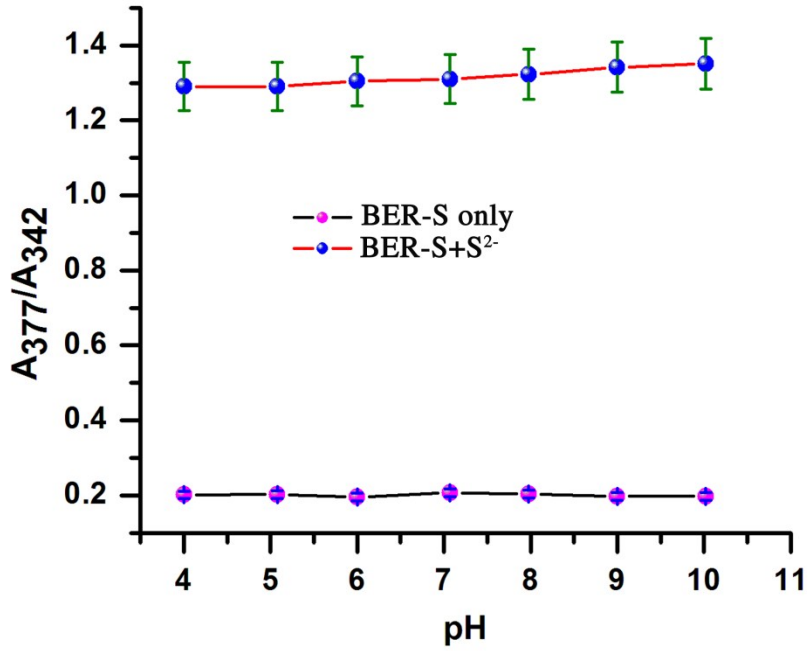

Fig. S8 Absorbance ratio (A_{377}/ A_{342}) of BER-S and BER-S + S^{2-} at various pH values.

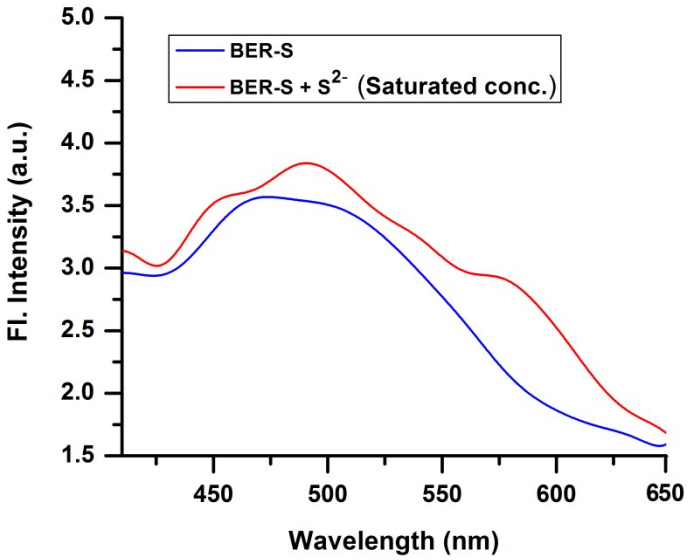

Fig. S9 Emission spectra of BER-S (10μM) and BER-S + S^{2-} (25 μM)

Sensing images by BER-S/ DNA complex colorimetrically:

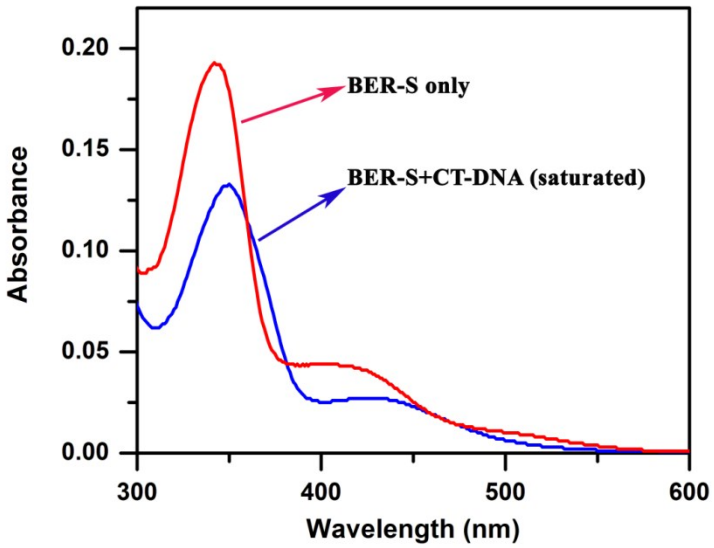

Fig. S10 UV-vis spectra of free BER-S (10μM) and BER-S (10μM) + CT-DNA (75μM) in CP buffer solution.

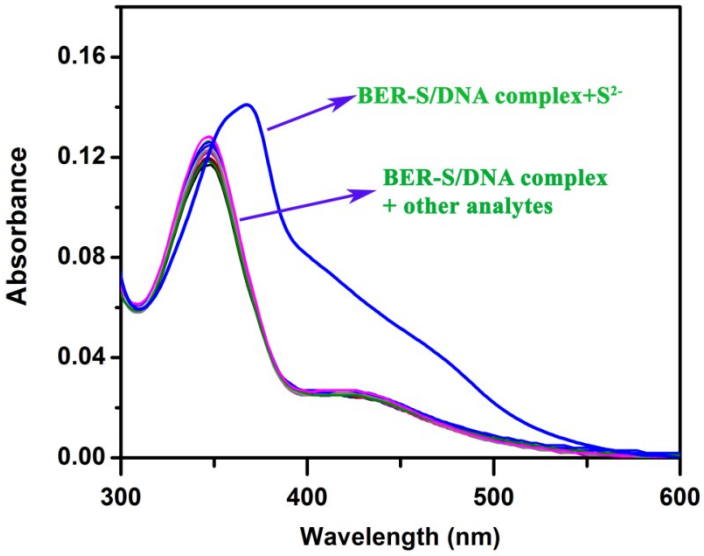

Fig. S11 UV-vis spectra of BER-S (10μM) + DNA (75 μM) in the presence of various analytes stated earlier.

Images of fluorometric sensing of S2- by BER-S/DNA complex:

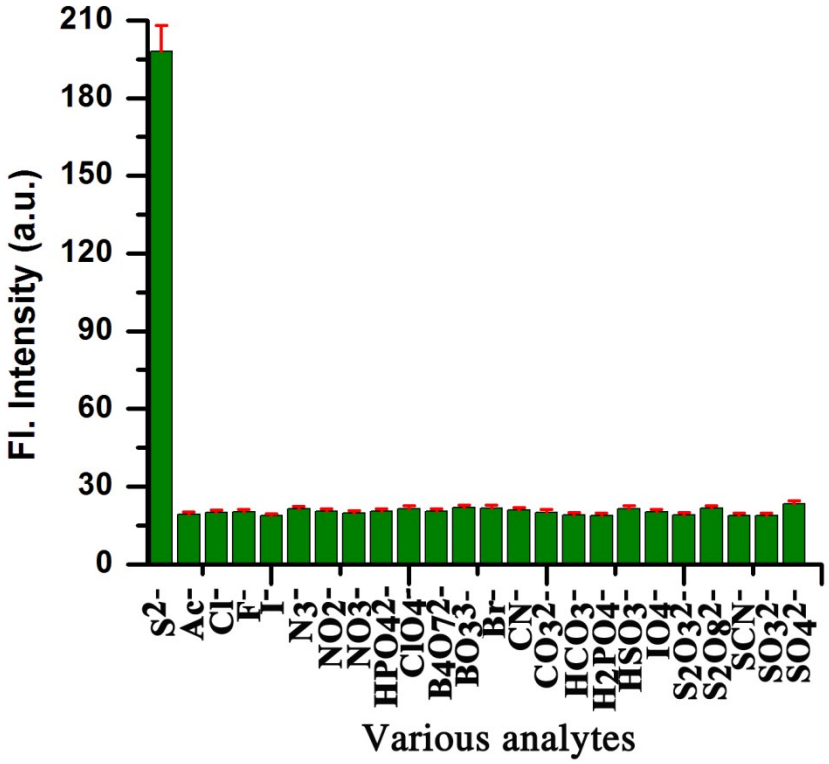

Fig. S12 Emission spectra of BER-S-DNA system (BER-S= 10 μM, DNA = 150 μM) in the presence various metal ions and anions (20 μM S^{2-}, Cl^{-}, Br^{-}, I^{-}, F^{-}, Ac^{-}, NO_2^{-}, NO_3^{-}, CN^{-}, SCN^{-}, HSO_3^{-}, SO_4^{2-}, SO_3^{2-}, $S_2O_3^{2-}$, $S_2O_8^{2-}$, HPO_4^{2-}, $H_2PO_4^{-}$, PO_4^{3-}, ClO_4^{-}, IO_4^{-}, $S_2O_8^{2-}$, BO_3^{3-}, $B_4O_7^{2-}$, N_3^{-}) in CP buffer solution, λex= 360 nm, λem= 530nm, measured after 20 min of mixing.

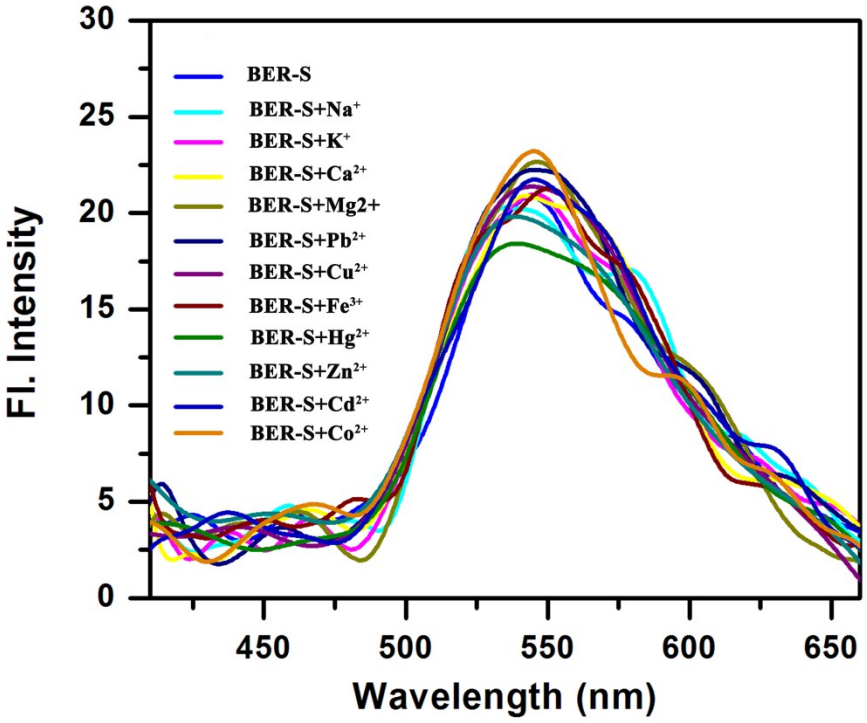

Fig. S13 Emission spectra of BER-S-DNA system (BER-S= 10 μM, DNA = 150 μM) in the presence various metal ions (20 μM of each, Na^{+}, K^{+}, Ca^{2+}, Mg^{2+}, Pb^{2+}, Cu^{2+}, Fe^{3+}, Hg^{2+}, Zn^{2+}, Cd^{2+}, Co^{2+}) in CP buffer solution, λex= 360 nm, λem= 530nm, measured after 20 min of mixing.

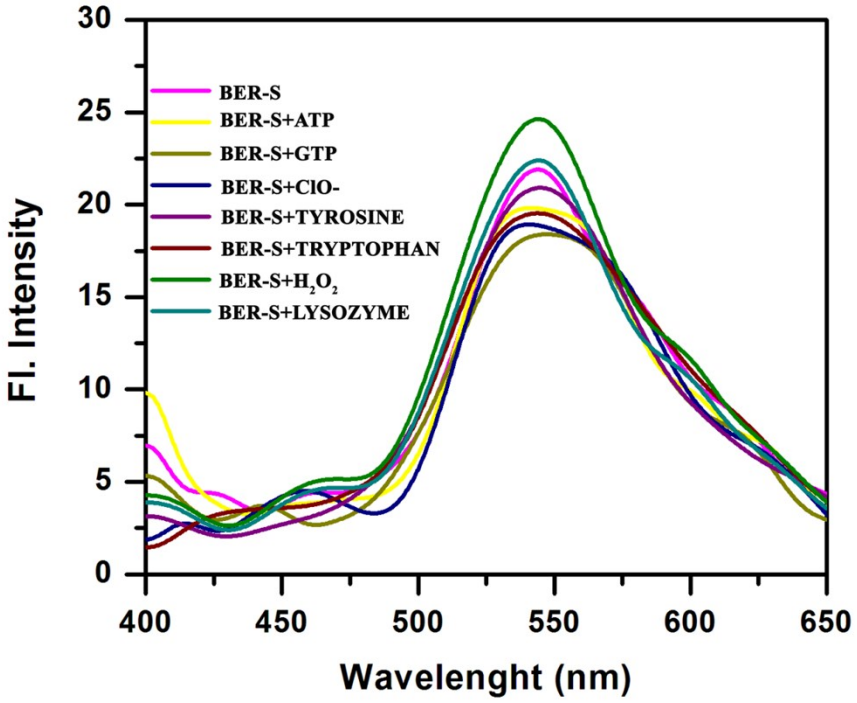

Fig. S14 Emission spectra of BER-S-DNA system (BER-S= 10 μM, DNA = 150 μM) in the presence various life elements (20 μM of each, ATP, GTP, ClO^-, H_2O_2, tyrosine, tryptophan, lysozyme) in CP buffer solution, λex= 360 nm, λem= 530nm, measured after 20 min of mixing.

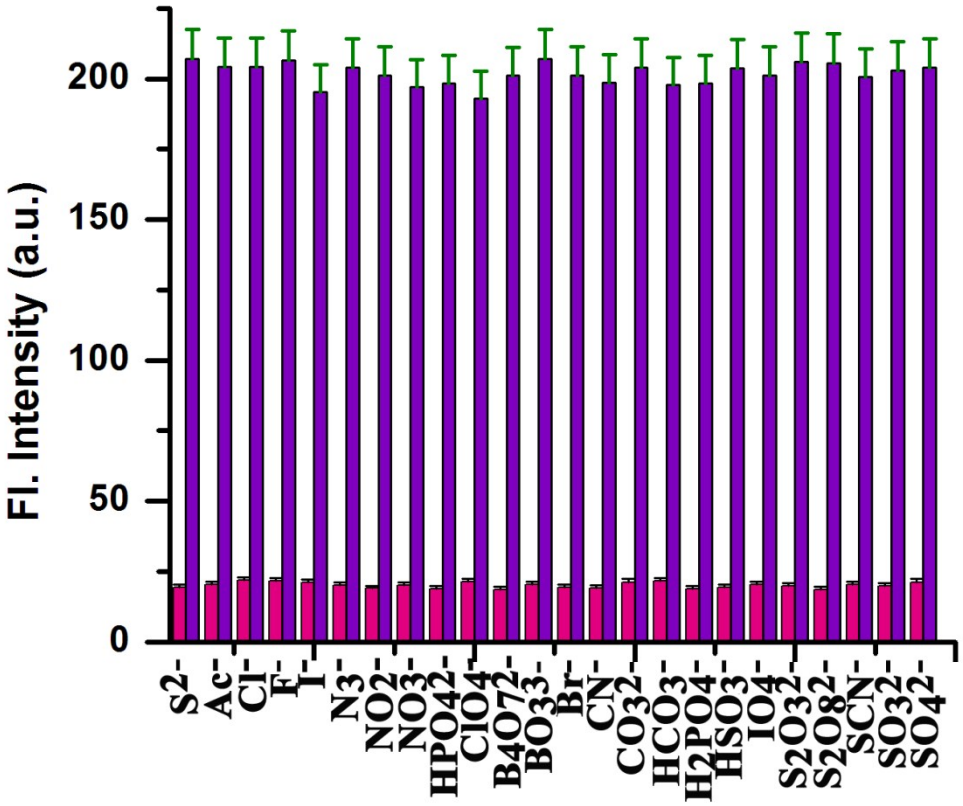

Fig. S15 Emission spectra of BER-S/DNA complex (10 μM and 150 μM) to various anion stated above in CP buffer (10 mM, pH = 7.4). The red bars represent the emission of probe in the presence of anions (each of 20μM). The violet bars signify the emission of the probe-analytes solution that occurs upon the consequent addition of 20μM of S^{2-} to the above solution.

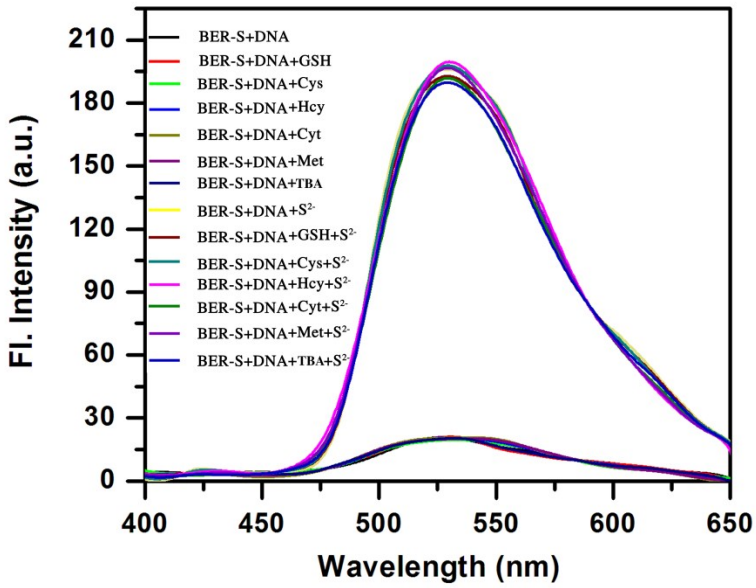

Fig. S116 Emission spectra of BER-S/DNA complex (10 μM and 150 μM) in the presence of various biothiols (20 μM for cysteine, homocysteine, glutathione, methionine, cysteamine and thiobarbituric acid) and emission spectra of BER-S/DNA complex- biothiols after addition of S^{2-} in CP buffer solution, measured after 25 min of mixing.

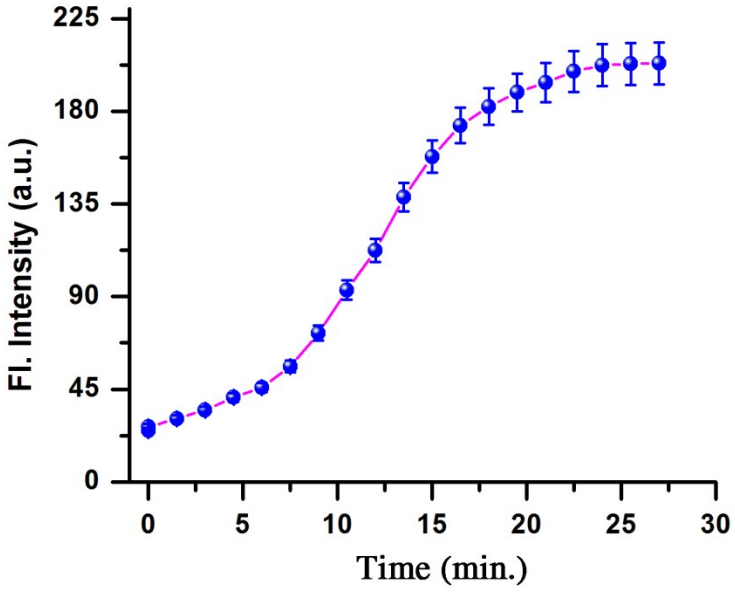

Fig. S17 Time-dependent emission spectra of BER-S/DNA complex with sulfide anion (20μM) in CP buffer solution.

Cell viability study of BER-S:

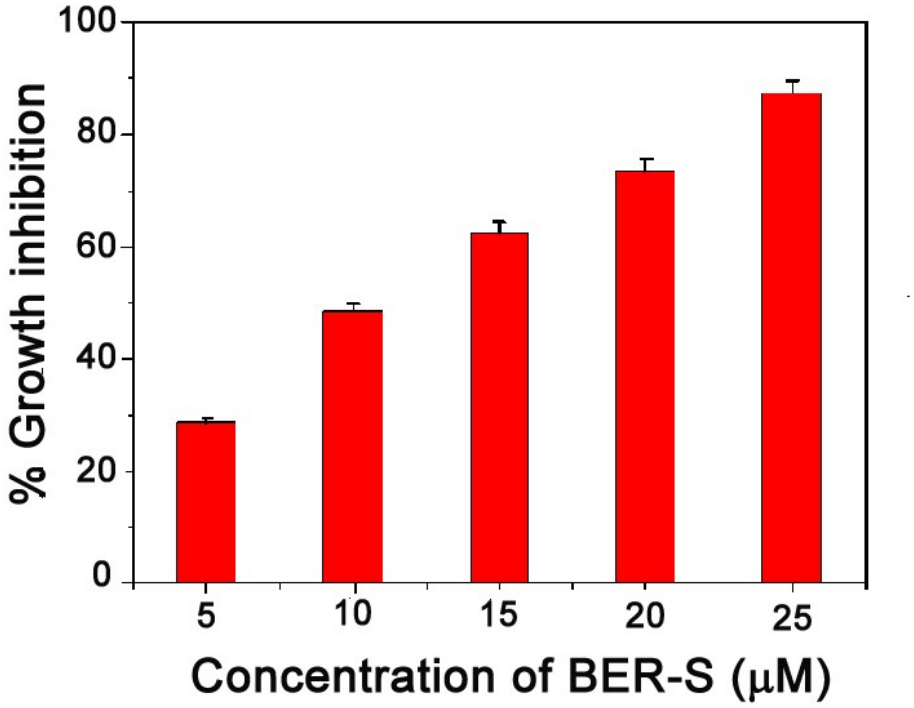

Fig. S18 MTT assay for the growth inhibition of skin melanoma cells treated with various concentrations of BER-S for 24 hours.

Computational Study:

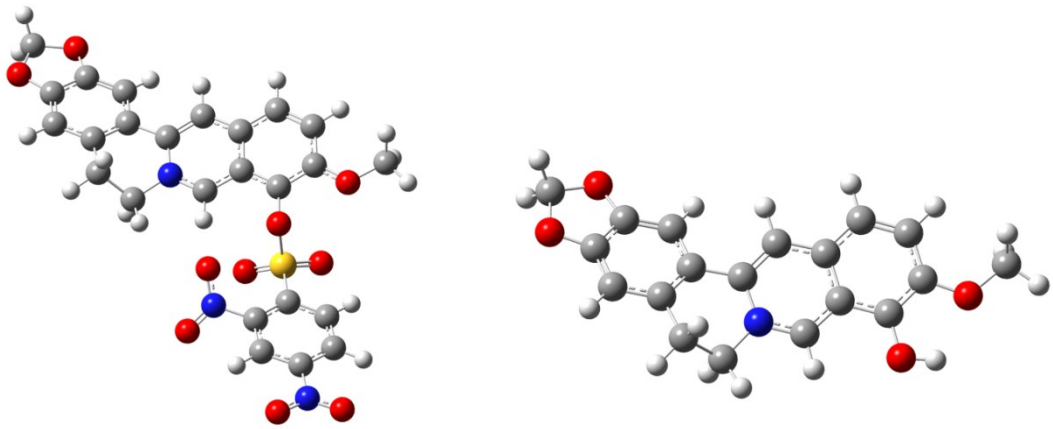

Fig. S19 The optimized conformation of BER-S and BER-OH in the ball and stick model; carbon, oxygen, nitrogen and sulfur atoms are colored in gray, red, blue and yellow respectively.

Table: S4 Calculation of HOMO – LUMO energy gap of reactant (BER-S) and product (BER-OH)

Entry	HOMO (eV)	LUMO (eV)	H_LGap(eV)
BER-S	-0.20959	-0.09374	3.15239435
BER-OH	-0.21597	-0.12881	2.37171076

Characterization of BER-S:

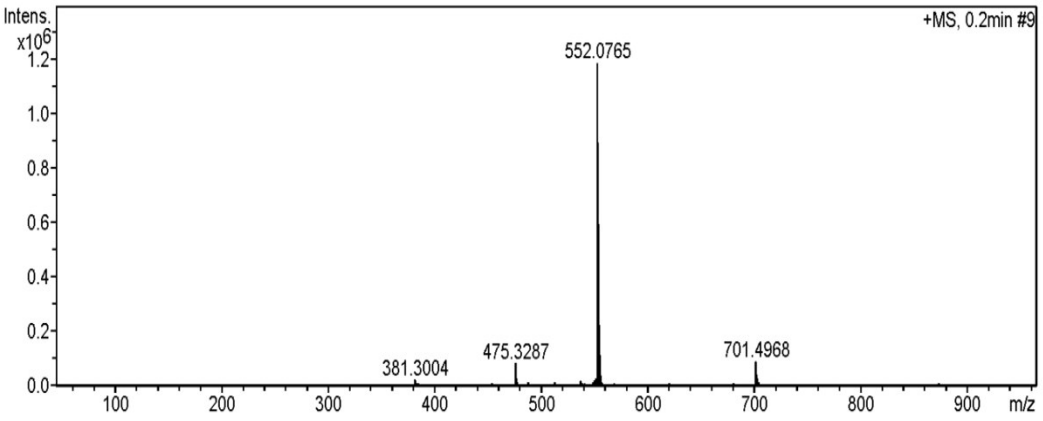

Fig. S20 HRLC- MS spectrum of BER-S.

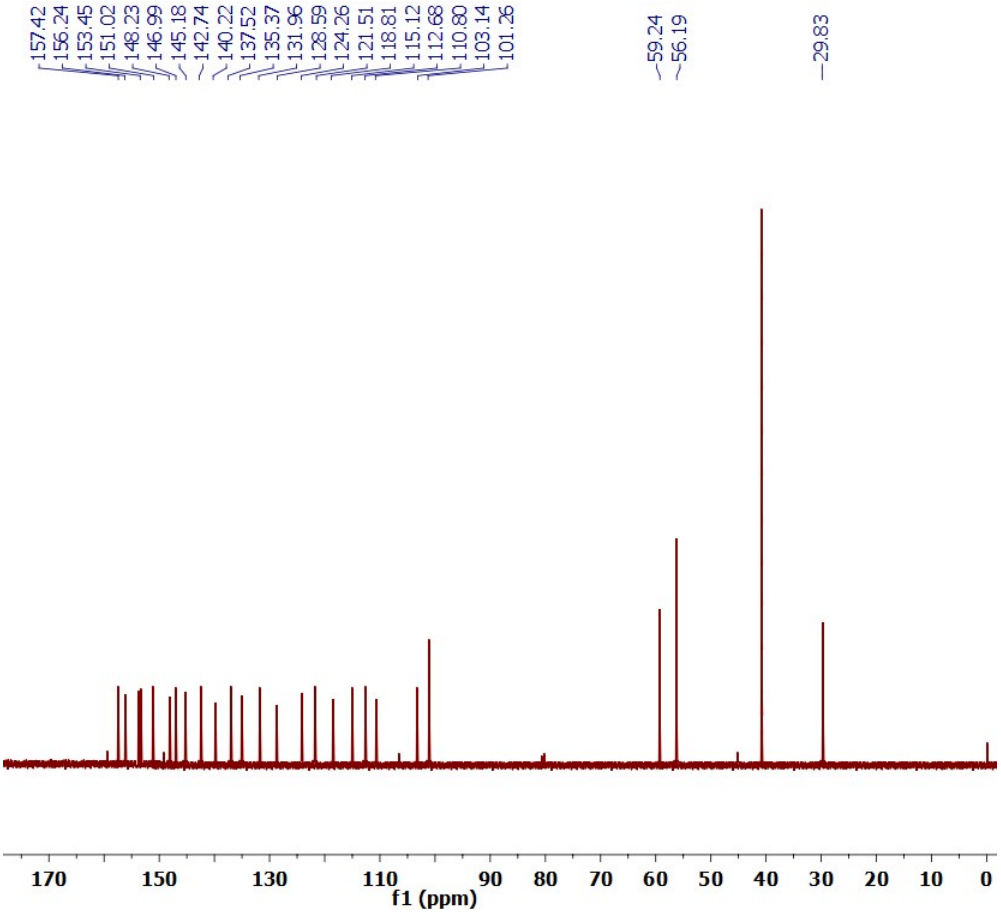

Fig. S 21 ^{13}C NMR spectra of BER-S in d_6-DMSO.

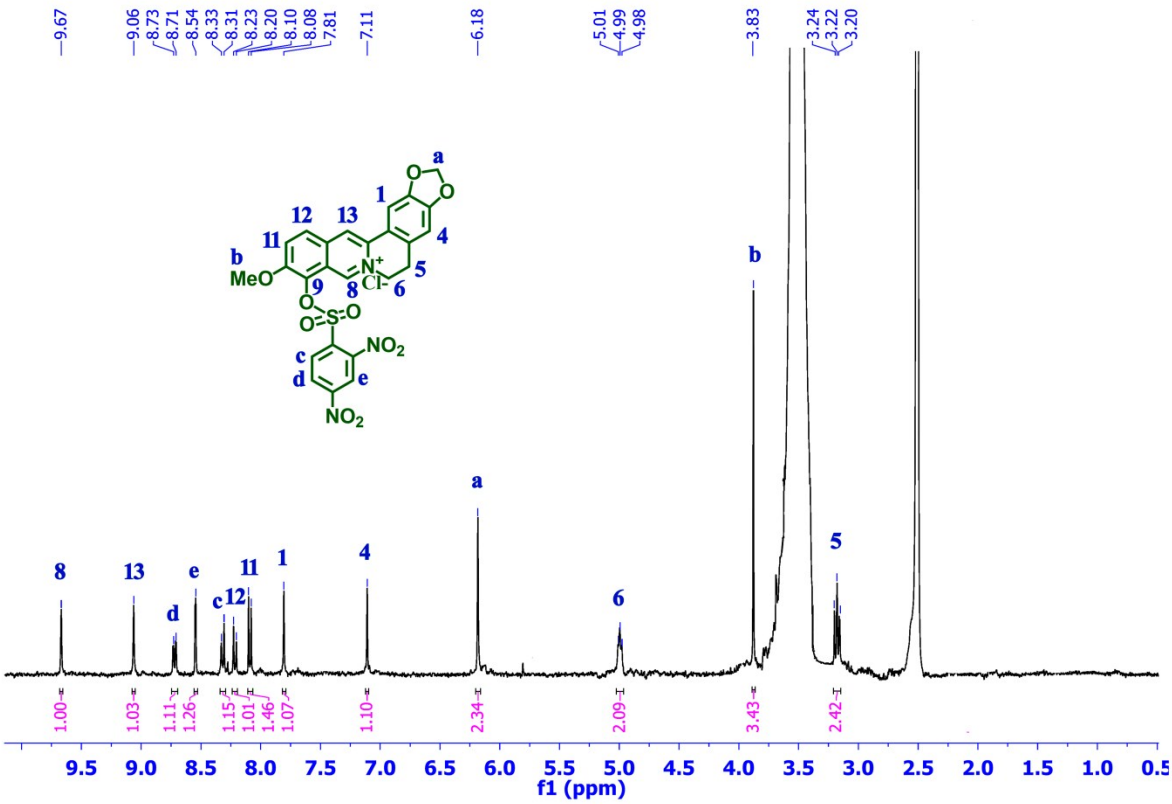

Fig. S22 ^{1}H NMR spectra of BER-S in d_6-DMSO.